Heterogeneous Interaction of H2O2 with Arizona Test Dust

ARTICLE *in* THE JOURNAL OF PHYSICAL CHEMISTRY A · DECEMBER 2013

Impact Factor: 2.69 · DOI: 10.1021/jp409946j · Source: PubMed

3 AUTHORS:

Atallah El Zein
Université du Littoral Côte d'Opale (ULCO)
13 PUBLICATIONS **119** CITATIONS
SEE PROFILE

Manolis N Romanias
Ecole des Mines de Douai
25 PUBLICATIONS **99** CITATIONS
SEE PROFILE

Yuri Bedjanian
CNRS Orleans Campus
67 PUBLICATIONS **853** CITATIONS
SEE PROFILE

THE JOURNAL OF PHYSICAL CHEMISTRY A

Article

pubs.acs.org/JPCA

Heterogeneous Interaction of H_2O_2 with Arizona Test Dust

Atallah El Zein, Manolis N. Romanias, and Yuri Bedjanian*

Institut de Combustion, Aérothermique, Réactivité et Environnement (ICARE), CNRS, 45071 Orléans Cedex 2, France

ABSTRACT: The heterogeneous interaction of H_2O_2 with solid films of Arizona Test Dust (ATD) was investigated under dark conditions and in presence of UV light using a low pressure flow tube reactor coupled with a quadrupole mass spectrometer. The uptake coefficients were measured as a function of the initial concentration of gaseous H_2O_2 ($[H_2O_2]_0$ = (0.18 − 5.1) × 10^{12} molecules cm^{-3}), irradiance intensity (J_{NO_2} = 0.002 − 0.012 s^{-1}), relative humidity (RH = 0.002 − 69%), and temperature (T = 268 − 320 K). The initial uptake coefficient was found to be independent of the concentration of H_2O_2 and UV irradiation intensity and to decrease with increasing RH and temperature according to the following expressions: $\gamma_0 = 4.8 \times 10^{-4}/(1+ RH^{0.66})$ at T = 275 K and $\gamma_0 = 3.2 \times 10^{-4}/(1 + 2.5 \times 10^{10}\exp(-7360/T))$ at RH = 0.35% (calculated using BET surface area, estimated conservative uncertainty of 30%). By contrast, the steady state uptake coefficient was found to be independent of temperature, to increase upon UV irradiation of the surface, and to be inversely ($\gamma_{SS} \sim [H_2O_2]^{-0.6}$) dependent on the concentration of H_2O_2. The RH independent steady state uptake coefficient was measured under dark and UV irradiation conditions: γ_{SS}(dark) = (0.95 ± 0.30) × 10^{-5} and γ_{SS}(UV) = (1.85 ± 0.55) × 10^{-5}, for RH = (2 − 69)% and $[H_2O_2]_0 \cong 1.0 \times 10^{12}$ molecules cm^{-3}. The present experimental data support current considerations that uptake of H_2O_2 on mineral aerosol is potentially an important atmospheric process.

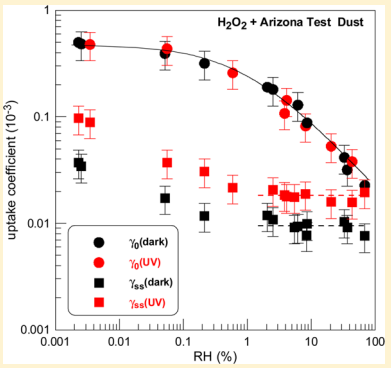

1. INTRODUCTION

Mineral dust is a significant component of atmospheric aerosols. According to recent estimations, 1600 Tg of mineral dust is released every year in the atmosphere.[1] Although the primary sources of dust particles are arid regions, due to the global air circulation, aerosol particles undergo long-range transportation to populated areas and influence the air quality and public health.[2,3] The dust surfaces provide the seedbed for adsorption−reaction of trace gas molecules, and therefore, are considered to play a key role in the transformation and environmental fate of many atmospheric species.[4,5]

Hydrogen peroxide is an important atmospheric species directly related to the chemistry of HO_x (OH + HO_2) radicals and oxidative capacity of the troposphere.[6,7] H_2O_2 is mainly formed via self-reaction of HO_2 radicals. The removal pathways of H_2O_2 are photolysis, reaction with OH, and dry/wet deposition:

$$H_2O_2 + h\nu(\lambda \leq 360\ nm) \rightarrow 2OH$$

$$H_2O_2 + OH \rightarrow HO_2 + H_2O$$

Therefore, the atmospheric concentration of H_2O_2 determined by its production and removal rates is affected by the levels of chemical components such as NO_x, CO, CH_4, and nonmethane hydrocarbons, and also by meteorological parameters such as solar radiation, water vapor concentration, temperature, and pressure.[8,9] As a result, the mixing ratios of H_2O_2 measured in the troposphere vary in a rather wide range, from a few tenths to nearly 10 ppbv.[10,11] In addition, due to the high water solubility, H_2O_2 is acting as an important oxidant of sulfur compounds in the aqueous phase and may play a potentially important role in the formation of secondary organic aerosols.[12]

Recent studies have shown that the large discrepancies between observed and modeled H_2O_2 concentrations in a Sahara dust plume and in the Arctic spring troposphere can be reduced, after incorporating into models the heterogeneous uptake of H_2O_2 and HO_2 on aerosol surfaces, revealing a crucial role of these processes in the tropospheric photochemistry.[13,14] In this respect, quantitative experimental data on the removal of H_2O_2 in heterogeneous reactions on aerosol surfaces are needed to clarify the impact of this process on HO_x budget, and consequently, on concentrations of ozone and other atmospheric pollutants. Available information on the kinetics of H_2O_2 interactions with mineral oxide surfaces is rather scarce and seems to be limited to a few recent studies,[15−20] realized under dark conditions. The experimental data on temperature and relative humidity dependence of the uptake coefficients of H_2O_2 are even more limited.

In recent studies from our group,[21,22] the heterogeneous interaction of H_2O_2 with three components of mineral aerosol, Al_2O_3, Fe_2O_3 and TiO_2, was investigated under dark and UV irradiation conditions. In the present study, we report the measurements of the uptake coefficient of H_2O_2 on Arizona Test Dust (ATD) under dark and UV irradiation conditions as a function of a number of parameters such as relative humidity, temperature, initial concentration of H_2O_2 and UV irradiation intensity. Arizona Test Dust is a mixture of metal oxides (Table

Received: October 7, 2013
Revised: November 26, 2013
Published: December 19, 2013

1) which are generally present in atmospheric mineral aerosols in various proportions.[23]

Table 1. Typical Chemical Composition of Arizona Test Dust

chemical	percent of weight
SiO_2	68−76%
Al_2O_3	10−15%
Fe_2O_3	2−5%
Na_2O	2−4%
CaO	2−5%
MgO	1−2%
TiO_2	0.5−1%
K_2O	2−5%

Analysis of the experimental data available for the uptake of atmospheric trace gases on different mineral surfaces reveals that ATD mimics quite well the reactivity of authentic dust samples. Indeed, for the uptake to ATD surface, uptake coefficients were identical to those on Saharan dust for NO_2 and NO_3; however, somewhat lower uptake coefficients (by a factor of 1.5−2) for N_2O_5 and HNO_3 were reported.[24]

2. EXPERIMENTAL SECTION

The measurements of the uptake of H_2O_2 to ATD surface were conducted in a coated rod flow tube reactor combined with a modulated molecular beam quadrupole mass spectrometer (Balzers, QMG 420) for the detection of the gas phase species. The experimental equipment and approach used for the kinetic measurements were described in previous publications from this group.[21,25,26] Briefly, the main reactor (Figure 1) consisted of a Pyrex tube (40 cm length and 2.4 cm i.d.) with a jacket for the thermostatted liquid circulation.

Experiments were carried out using a coaxial configuration of the flow reactor, a Pyrex tube with the outer mineral coating being introduced into the main reactor along its axis. The coated tube could be moved, which allowed the variation of the solid film length exposed to gas phase reactant and consequently the variation of the reaction time (Figure 1). The temperature of the sample could be changed by two methods: by circulating thermostatted water or ethanol inside the tube coated with the sample or by means of a coaxial cylindrical heater (5 mm o.d., 20 cm length), which could be introduced inside the support tube. The reactor was surrounded by 6 UV lamps (Sylvania BL350, 8 W, 315−400 nm with peak at 352 nm). The irradiance intensity in the reactor was characterized by direct measurements of the NO_2 photolysis frequency, J_{NO2}, as a function of the number of lamps switched on. The values of J_{NO2} were found to be between 0.002 and 0.012 s^{-1} for 1 to 6 lamps switched on, respectively.[26]

Solid films of ATD were deposited on the outer surface of a Pyrex tube (0.9 cm o.d.) using a suspension of ATD (Powder Technology Inc., nominal 0−3 μm ATD) in ethanol. The support tube was immersed into the suspension, withdrawn, and dried with a fan heater. As a result, rather homogeneous (to the eye) solid films were formed at the Pyrex surface. In order to eliminate the possible residual traces of ethanol, prior to uptake experiments, the freshly prepared ATD samples were heated at 100−150 °C for 20−30 min under pumping. At the end of the kinetic experiments, the deposited solid sample was mechanically removed, and its mass was measured using a high-accuracy mass balance. BET surface area of the ATD powder was determined using a Quantachrome Autosorb-1-MP-6 apparatus, and nitrogen as adsorbate gas and was found to be 85 ± 10 m^2g^{-1}. It was verified that the BET surface area of ATD powder did not change during preparation of ATD films: similar (within 15%) specific surface areas were measured for the original (not treated) powder and that removed from the support tube.

The H_2O_2 vapor was delivered to the reactor by flowing He through the aqueous solution of H_2O_2 (60% wt H_2O_2/H_2O). The absolute calibration of the mass spectrometer for H_2O_2 was performed by injecting known amounts (0.5−10 μL) of the 60% wt solution inside the flow tube, and recording the parent mass peak intensity of H_2O_2 at m/z = 34. The integrated area of the mass spectrometric signals corresponding to a known total number of H_2O_2 molecules injected into the reactor allowed the determination of the calibration factor. The H_2O vapor was introduced into the flow reactor by passing Helium through a thermostatted (20 − 30 °C) glass bubbler containing deionized water. The concentrations of water vapor were determined by calculating the H_2O flow rate from the total (H_2O + He) and H_2O vapor pressures in the bubbler and the measured flow rate of He through the bubbler. The partial pressure of water vapor in the bubbler was measured with a VAISALA DRYCAP DMT340 dew-point transmitter. The estimated uncertainties on the determination of $[H_2O_2]$ and RH were nearly 15%.

3. RESULTS

3.1. Kinetics of H_2O_2 Uptake. Figure 2 shows a typical experimental sequence, during which initial concentration of H_2O_2 is first established in the reactor and then the ATD coated tube is introduced into the reaction zone (sample in). Upon contact with the reactive surface, the concentration of H_2O_2 initially drops, then increases to a steady level. Turning on the lamps (UV on) leads to a decrease of the steady state

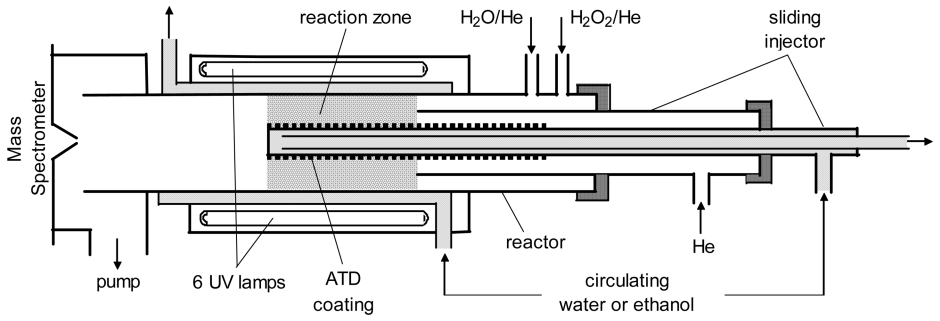

Figure 1. Diagram of the flow photoreactor.

dx.doi.org/10.1021/jp409946j | J. Phys. Chem. A 2014, 118, 441−448

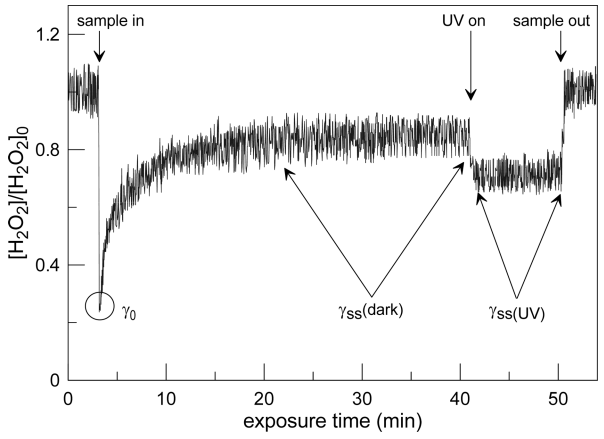

Figure 2. Typical uptake profiles of H_2O_2 concentration on ATD surface: dry conditions, T = 300 K, P = 1 Torr, $[H_2O_2]_0 = 5 \times 10^{11}$ molecules cm^{-3}, sample mass = 0.5 mg cm^{-1} × 6 cm.

concentration of H_2O_2 indicating a photoenhancement (about twice) of the H_2O_2 uptake on mineral dust. Finally, when the reactive surface is withdrawn from the reaction zone (sample out), that is when H_2O_2 is no longer in contact with the sample surface, the concentration of H_2O_2 recovers rapidly to its initial value. Reference experiments have shown that uptake of H_2O_2 on uncovered support tube was negligible. This could be expected, as, first, the surface (geometric one) of the clean Pyrex injector is too low (generally, 2 orders of magnitude lower) compared with that of ATD powder, and, second, SiO_2 is less reactive compared to other mineral oxides (see Discussion section). The effect of UV irradiation was observed only in the presence of ATD sample in contact with H_2O_2. It was verified that turning on the lamps in the absence of the reactive surface did not affect the concentration of H_2O_2 flowing through the reactor, indicating that photolysis of H_2O_2 in the gas phase was negligible.

In the present study, we have measured both initial (γ_0) and steady state uptake coefficients (γ_{SS}) of H_2O_2 on ATD surface under dark and UV irradiation conditions as shown in Figure 2. The uptake coefficient of H_2O_2 was determined as the probability of H_2O_2 loss per collision with the reactive surface:

$$\gamma = \frac{4k'}{\omega} \times \frac{V}{S} \qquad \text{(I)}$$

where k' is the first order rate constant of H_2O_2 loss (s^{-1}), ω the average molecular speed (cm s^{-1}), V the volume of the reaction zone (cm^3) and S the surface area of the solid sample involved in the heterogeneous reaction (cm^2). The rate constant of H_2O_2 loss was determined from the exponential decays of H_2O_2 as

$$k'_{obs} = -\frac{d\ln([H_2O_2])}{dt} \qquad \text{(II)}$$

where k'_{obs} is the observed first order rate constant of the heterogeneous loss of H_2O_2, and t is the reaction time defined by the ratio of the sample length to the flow velocity in the reactor (the flow velocities were in the range 155−2580 cm s^{-1}). The values of the observed first-order rate constants, k'_{obs}, were corrected for the diffusion limitation in the H_2O_2 radial transport from the volume to the reactive surface using the expression (III) derived by Gershenzon and co-workers[27,28] for coaxial configuration of the reactor used in the present study:

$$\frac{1}{k'_{obs}} = \frac{1}{k'} + \frac{R^2}{K^d(q)D_0} \times P \qquad \text{(III)}$$

where k' is the true rate constant, D_0 is the diffusion coefficient of H_2O_2 at 1 Torr pressure (Torr cm^2 s^{-1}), P is the total pressure in the reactor in Torr, and $K^d(q)$ is a dimensionless rate constant of radial diffusion, which is a function of the sample tube outer radius (r) to main reactor inner radius (R) ratio, $q = r/R$. For the configuration used in the present study, q = 0.375 and $K^d(q)$= 4.4.[27] Diffusion corrections on k'_{obs} were calculated using expression III with D_0 = 415 Torr cm^2 s^{-1} determined in our recent study[19] and assuming $T^{1.75}$-dependence of D_0 on temperature. The corrections applied to k'_{obs} ranged from a few percents up to factor 1.8 (for the highest values of k'_{obs}).

3.2. Dependence on Coating Thickness. In order to determine the surface area of the solid samples involved in the interaction with H_2O_2, the loss rate of H_2O_2 was measured as a function of coating thickness.

The results of the measurements carried out at room temperature and under dry conditions are shown in Figure 3 as

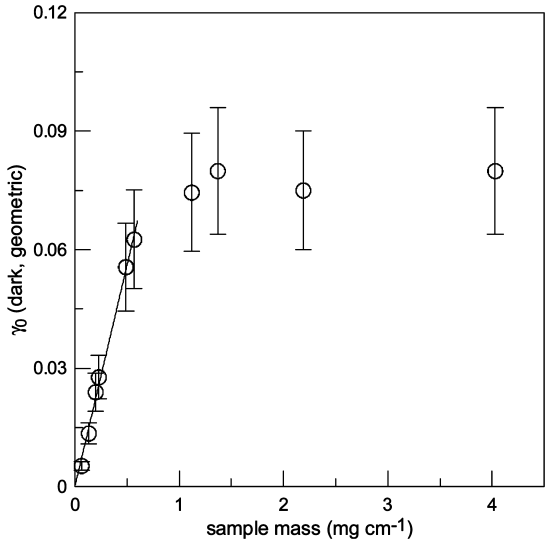

Figure 3. Initial uptake coefficient of H_2O_2 (calculated using geometric surface area) as a function of coating mass (per 1 cm length of the support tube): dry dark conditions, T = 300 K, P = 1 Torr, $[H_2O_2]_0 = 5.4 \times 10^{11}$ molecules cm^{-3}.

a dependence of the initial uptake coefficient of H_2O_2 (calculated with geometric "projected" surface area) on the mass of ATD powder deposited per length unit of the support tube (which is equivalent to the thickness of the coating). It can be seen that two regimes were observed: the first one, where the geometric uptake coefficient linearly increases upon increase of sample mass, and the second one, where it is mass-independent. The linear relationship between the reaction probability (geometric) and mass (thickness) of the reactive film was considered as an indication that the entire surface area of the solid sample is accessible to H_2O_2.[29] The uptake measurements in the present study were carried out with dust samples with masses below 0.6 mg cm^{-1}, where linear dependence of the reaction rate on sample mass was observed, and BET surface area (85 m^{2}g^{-1}) was used to determine γ.

dx.doi.org/10.1021/jp409946j | J. Phys. Chem. A 2014, 118, 441−448

The linear dependences in Figure 3 provide the following value for the initial uptake coefficient of H_2O_2 under dry conditions (RH ≈ 0.0025%) and T = 300 K:

$$\gamma_0(\text{dark}) = (3.8 \pm 1.1) \times 10^{-4}$$

where estimated (nearly 30%) uncertainty represents a combined error on determination of the surface area and measurements of k'. It is worth mentioning that the values obtained for γ, calculated with BET surface area, should be considered as a lower limit of the uptake coefficient.

3.3. Dependence on Initial Concentration of H_2O_2. The dependence of the uptake coefficient on initial concentration of H_2O_2 in the gas phase was studied for $[H_2O_2]_0$ varied between 1.8×10^{11} and 5.1×10^{12} molecules cm^{-3}. Experiments have been performed at T = 300 K, dry conditions and 1 Torr total pressure in the reactor. The results obtained for γ_0(dark) and γ_{SS}(dark) are displayed in Figure 4.

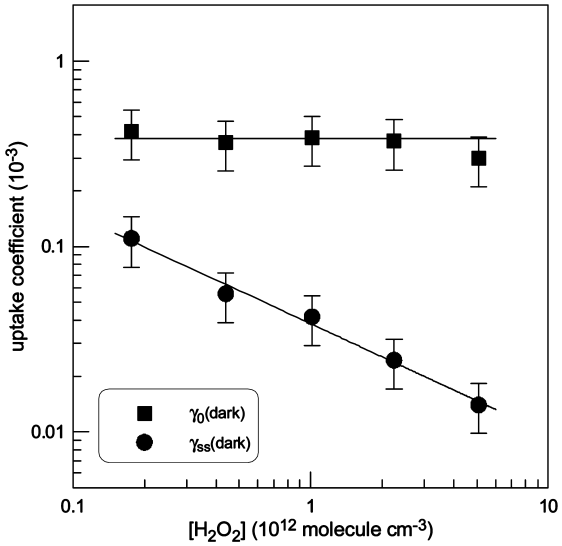

Figure 4. Uptake coefficient as a function of initial H_2O_2 concentration: dry conditions, T = 300 K, P = 1 Torr. The error bars reflect the estimated uncertainties of 30% on determination of the uptake coefficients.

The initial uptake coefficient can be considered independent of $[H_2O_2]_0$ in the explored range of H_2O_2 concentrations. Independence of the initial uptake of $[H_2O_2]$ could be expected since, at the initial stage of the surface exposure, the active sites on the surface are not depleted or blocked and are all available for the heterogeneous reaction. Regarding the steady state uptake coefficient, an inverse dependence of γ_{SS}(dark) on $[H_2O_2]_0$ was observed in the whole range of H_2O_2 concentrations used according to the following empirical expression:

$$\gamma_{SS}(\text{dark}) = 3.8 \times 10^{-5} \times ([H_2O_2]_0)^{-0.6}$$

where concentration of H_2O_2 is in 10^{12} molecules cm^{-3} units. The inverse dependence of the steady state uptake on concentration of H_2O_2 is probably due to the surface saturation with the adsorbed precursor.

3.4. Dependence on RH and UV Irradiation Intensity. The uptake coefficient of H_2O_2 was measured at T = 275 K with relative humidity varied between 0.002 and 69%. The choice of the relatively low temperature in these experiments was driven by the need to ensure high levels of RH, relevant for the atmosphere, inside our low pressure flow reactor (P = 1 − 9 Torr). Prior to exposure to H_2O_2, the freshly prepared mineral samples were exposed during nearly 5 min to water vapor present in the reactor. Longer (up to 30 min) exposure of samples to water vapor had no impact on the observed uptake data, indicating that water to surface adsorption equilibrium was reached after a few minutes. The RH-dependence of the initial and steady state uptake coefficients measured under dark and UV irradiation conditions (6 lamps on) is displayed in Figure 5.

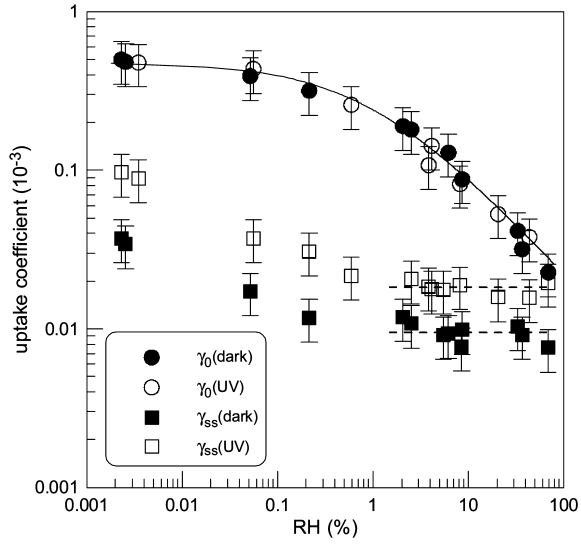

Figure 5. Uptake coefficient of H_2O_2 as a function of relative humidity, under dark conditions and on UV irradiated (6 lamps) surface: T = 275 K, P = 1 − 9 Torr, $[H_2O_2]_0 \approx 1.0 \times 10^{12}$ molecules cm^{-3}.

One can note that, in the range of the experimental uncertainty, similar values of γ_0 were observed under dark conditions and in the presence of UV irradiation. The solid line in Figure 5 corresponds to the following empirical equation:

$$\gamma_0 = 4.8 \times 10^{-4}/(1 + \text{RH}^{0.66})$$

which describes quite well the experimental data for the initial uptake (with estimated conservative uncertainty of 30%) in the whole RH range used. Figure 5 also demonstrates the RH-dependence of the steady state uptake coefficient observed under dark and UV irradiation conditions (with $[H_2O_2]_0 \cong 1.0 \times 10^{12}$ molecules cm^{-3}). The measured steady state uptake coefficients can be considered as independent of relative humidity in the range RH = (2 − 69)% with values:

$$\gamma_{SS}(\text{dark}) = (0.95 \pm 0.30) \times 10^{-5}$$

$$\gamma_{SS}(\text{UV}) = (1.85 \pm 0.55) \times 10^{-5}$$

(with 6 lamps turned on)

The observed decrease of the initial uptake coefficient upon increase of RH points to the role of water rather as blocking the available active sites on the surface of ATD and seems to be in line, at least qualitatively, with the available data for the adsorption of water on mineral oxides.[30,31] Indeed, it was reported that water adsorption to SiO_2, Al_2O_3, MgO, Fe_2O_3, and TiO_2 (which are components of ATD) could be well

dx.doi.org/10.1021/jp409946j | J. Phys. Chem. A 2014, 118, 441−448

described with the Brunauer–Emmett–Teller (BET) type isotherm, with the monolayer coverage occurring between 20 and 30% relative humidity.[30,31] Independence of the steady state uptake coefficient of relative humidity observed at elevated RH indicates that a part (although a small one) of the surface reactive sites retains its reactivity even in the presence of a monolayer of adsorbed water. One can note that an increase of γ_{SS} was observed upon UV irradiation of the reactive surface. This effect is most probably due to the presence of 0.5–1% of TiO_2 in ATD, for which relatively high value of $\gamma_{SS}(UV) \sim 3.5 \times 10^{-3}$ was reported previously.[21] The absence of irradiation impact on the initial uptake coefficient can be explained by a delayed photoactivation of the reactive surface, as observed previously.[21]

The dependence of $\gamma_{SS}(UV)$ on the intensity of UV irradiation was explored in additional experiments by switching on different number of lamps in the reactor, from 1 to 6. This corresponds to the variation of the NO_2 photolysis frequency from 0.002 to 0.012 s^{-1}. Under these irradiance conditions, a linear relationship between $\gamma_{SS}(UV)$ and irradiation intensity was observed (Figure 6) pointing to the photocatalytic nature

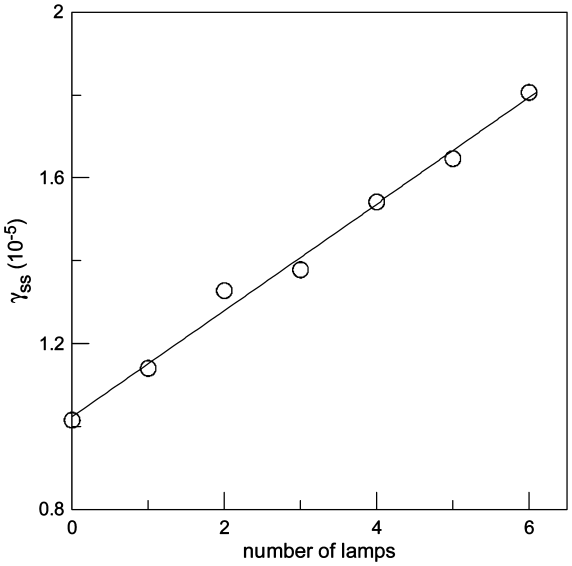

Figure 6. Steady state uptake coefficient as a function of the UV irradiation intensity: P = 9 Torr, T = 300 K, RH = 2.3%, $[H_2O_2]_0 \approx 1.0 \times 10^{12}$ molecules cm^{-3}, $J_{NO_2} = 0 - 0.012$ s^{-1} (0–6 lamps).

of the heterogeneous reaction. It can be noted that the range of values of J_{NO2} between 0.002 and 0.012 s^{-1} corresponding to 1 to 6 lamps switched on in the reactor overlaps with the values of J_{NO_2} measured in the atmosphere under cloud and clear sky conditions.[32]

It should be noted that experiments with UV irradiated ATD were carried out in the absence of oxygen in the reactive system. In the presence of O_2, which is an efficient scavenger of electrons on the photocatalyst surface, the photochemistry of H_2O_2 on mineral surface can be different. Unfortunately, the experimental system used in this study is not suitable for use under high concentrations of O_2.

3.5. Temperature Dependence. Temperature dependence of the initial uptake coefficients was measured in the temperature range (268–320) K with initial concentration of $H_2O_2 \approx 1.0 \times 10^{12}$ molecules cm^{-3} at a fixed relative humidity, RH ≈ 0.35%. The results are presented in Figure 7. As one can note, the initial uptake coefficient was found to be constant at lower temperatures (268–280 K) and to decrease with increasing temperature.

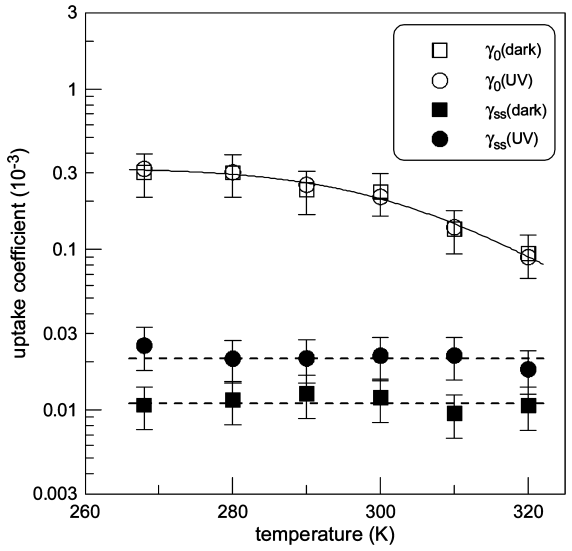

Figure 7. Uptake coefficient of H_2O_2 as a function of temperature: P = 1–9 Torr, T = 268 – 320 K, RH = (0.3–0.4) %, $[H_2O_2]_0 \approx 1.0 \times 10^{12}$ molecules cm^{-3}, irradiation with 6 lamps.

The solid line in Figure 7 fits the experimental data according to the following expression:

$$\gamma_0 = 3.2 \times 10^{-4}/(1 + 2.5 \times 10^{10} \exp(-7360/T))$$

$$\text{at RH} = 0.35\%$$

A similar temperature dependence of γ_0 was observed in our recent study of the interaction of H_2O_2 with Al_2O_3 and Fe_2O_3 surfaces.[22] It was speculated that the unusual and rather strong dependence of γ_0 on temperature could be due to the competition between surface reaction of H_2O_2 and its desorption. In fact, the expression for γ (T) similar to that given above can be derived from a simplified mechanism implying H_2O_2 adsorption (k'_{ads}), desorption (k'_{des}) and surface reaction (k'_r). Assuming a steady concentration of H_2O_2 on the surface, the net rate of H_2O_2 loss in the gas phase can be expressed as $k' = k'_{ads}/(1 + k'_{des}/k'_r)$. In the frame of this interpretation, the T-factor in the above expression for γ_0 corresponds to the difference between activation energies for desorption and surface reaction. On the other hand, the observed temperature dependence of the uptake coefficient may also reflect the possible dependence of γ_0 on absolute concentration of water. One can note the resemblance between temperature and RH dependence of the uptake coefficient. The temperature dependence was measured at fixed relative humidity of 0.35%. It means that the absolute concentration of water in the reactor was different at different temperatures. For example, the concentration of water at T = 280 K was by nearly 1 order of magnitude lower than at 320 K. Taking into account these considerations, the expression for the temperature dependence of γ_0 should be viewed as an empirical one without any physical meaning, as it just allows us to describe our results in the temperature range used.

In contrast to the initial uptake data, the steady state uptake was found to be independent of temperature in the T-range used. The dashed lines in Figure 7 correspond to the following

dx.doi.org/10.1021/jp409946j | J. Phys. Chem. A 2014, 118, 441–448

Table 2. Summary of the Literature Data for the Initial Uptake Coefficient (γ_0) of H_2O_2 on Mineral Oxides

reference	substrate	$[H_2O_2]$, 10^{12} molecules cm^{-3}	RH, %	T, K	γ_0
Wang et al.[17]	α-Al_2O_3	0.1−2.5	dry	298	1.0×10^{-4}
	MgO	0.1−0.6	dry	298	1.7×10^{-4}
	Fe_2O_3	0.1−2.5	dry	298	9.7×10^{-5}
	SiO_2	0.1−2.5	dry	298	5.2×10^{-5}
Zhou et al.[19]	SiO_2	0.8	dry	253−313	$\exp(934.5/T - 12.7)/(1 + \exp(934.5/T - 12.7))$
	$CaCO_3$	0.8	dry	253−313	$\exp(1193/T - 11.9)/(1 + \exp(1193/T - 11.9))$
Romanias et al.[22a]	γ-Al_2O_3	0.15−10	0.002−73	280	$1.10 \times 10^{-3}/(1 + RH^{0.93})$
			0.3	268−320	$8.7 \times 10^{-4}/(1 + 5.0 \times 10^{13} \exp(-9700/T))$
	Fe_2O_3	0.15−10	0.002−73	280	$1.05 \times 10^{-3}/(1 + RH^{0.73})$
			0.3	268−320	$9.3 \times 10^{-4}/(1 + 3.6 \times 10^{14} \exp(-10300/T))$
Pradhan et al.[15]	TiO_2	4.1	15−70	295	$1.5 \times 10^{-3} - 5.0 \times 10^{-4}$
Romanias et al.[21]	TiO_2	0.2−1.0	0.003−82	275	$4.1 \times 10^{-3}/(1 + RH^{0.65})$
Pradhan et al.[16]	Gobi dust	3.5−8.2	15−70	295	$3.3 \times 10^{-4} - 6.0 \times 10^{-4}$
	Saharan dust	3.5−8.2	15−70	295	$6.2 \times 10^{-4} - 9.4 \times 10^{-4}$
This study[a]	ATD	0.18−5.1	0.002−69	275	$4.8 \times 10^{-4}/(1 + RH^{0.66})$
			0.35	268−320	$3.2 \times 10^{-4}/(1 + 2.5 \times 10^{10} \exp(-7360/T))$

[a]The reported uptake coefficients are independent of the UV irradiation intensity ($J_{NO_2} = 0 - 0.012$ s^{-1})

values of γ_{SS} under dark conditions and UV irradiated (6 lamps on) surface of ATD: $\gamma_{SS}(\text{dark}) = 1.1 \times 10^{-5}$ and $\gamma_{SS}(\text{UV}) = 2.1 \times 10^{-5}$ for $T = 268 - 320$ K, RH = (0.3 − 0.4)% and $[H_2O_2]_0 \cong 1.0 \times 10^{12}$ molecules cm^{-3}.

4. DISCUSSION

This is the first study of the interaction of H_2O_2 with Arizona Test Dust. However the present results can be compared with the data on H_2O_2 uptake to other mineral surfaces. Previous results on the initial uptake coefficients of H_2O_2 on mineral dust are presented in Table 2 for comparison purposes. In the study of Wang et al.[17] that employed a Knudsen cell reactor, the initial uptake coefficients of H_2O_2 on α-Al_2O_3, MgO, Fe_2O_3, and SiO_2 under dry conditions were reported: $\gamma_0 = 1.0 \times 10^{-4}$, 1.7×10^{-4}, 9.7×10^{-5}, and 5.2×10^{-5}, respectively. It can be noted that the uptake data reported by these authors for Al_2O_3 and Fe_2O_3 are by 1 order of magnitude lower than the corresponding values measured under dry conditions by Romanias et al.[22] The reason for this disagreement is not clear. In both studies, the dependence of γ_0 on thickness of mineral coating was explored and BET surface area was used for calculations of the uptake coefficients.

It can be seen that the absolute values of γ_0 measured on ATD surface in the present study are lower than those measured on the individual components of the dust, Al_2O_3, Fe_2O_3,[22] and TiO_2.[15,21] This observation might have been expected, given that ATD contains nearly 70% of relatively inactive SiO_2.

The rather strong temperature dependence observed for H_2O_2 uptake to ATD is very similar to those reported in a previous study from our group for Al_2O_3 and Fe_2O_3 surfaces.[22] Zhou et al.[19] investigated the interaction of H_2O_2 with SiO_2 and $CaCO_3$ surfaces over the temperature range from 253 to 313 K using a Knudsen cell reactor. Their observed uptake of H_2O_2 to these minerals was reported to be a nonreactive reversible adsorption/desorption process. The initial uptake coefficients were found to decrease by nearly a factor 2 with increase of temperature, being in the range $1.3 \times 10^{-4} - 6.1 \times 10^{-5}$, and $7.1 \times 10^{-4} - 3.0 \times 10^{-4}$ for SiO_2 and $CaCO_3$, respectively. From the derived thermochemical data, it was concluded that the adsorbed H_2O_2 is only weakly bound to SiO_2 and $CaCO_3$ surfaces, the estimated activation energies for desorption of H_2O_2 from SiO_2 and $CaCO_3$ being (9.15 ± 0.11) and (5.9 ± 0.9) kJ mol^{-1}, respectively.[19] The stronger negative temperature dependence observed for the uptake of H_2O_2 to ATD (present study), Al_2O_3 and Fe_2O_3[22] seems to point to rather chemical nature of H_2O_2 adsorption on these reactive surfaces in contrast to physical molecular adsorption occurring on nonreactive SiO_2 and $CaCO_3$ surfaces.

The initial uptake coefficient of H_2O_2 to the ATD surface was found to not change significantly under the lowest RH of the study (<0.1%), while in the RH range between 0.1 and 69%, a substantial decrease of γ_0 was observed. A similar inverse dependence of γ_0 on relative humidity was observed in previous studies for the interaction of H_2O_2 with Al_2O_3, Fe_2O_3[22] and TiO_2.[15,21] The negative dependence of the uptake coefficient on RH can be attributed to competition between water and hydrogen peroxide molecules for the available active sites on the reactive surface. By contrast, a positive correlation of the uptake coefficient with RH has been observed for the interaction of hydrogen peroxide with authentic Gobi and Saharan dust aerosol particles.[16] The promoting effect of water on H_2O_2 uptake to authentic dust samples was attributed to enhanced adsorption of H_2O_2 into water islands formed on the relatively inactive (compared with TiO_2) major components of the authentic dust (silica/alumina).[16] This hypothesis seems to be not supported by the uptake data for Al_2O_3,[18,22] Fe_2O_3[22] and SiO_2[18] showing a negative dependence of H_2O_2 uptake on relative humidity.

Comparison of the present data for ATD with those for Gobi and Saharan dust[16] reveals that not only RH behavior but also the absolute values of γ_0 measured on these surfaces are very different. Pradhan et al.[16] reported $\gamma_0 = 3.3 \times 10^{-4}$ at 15% RH rising to 6.0×10^{-4} at 70% RH for Gobi dust and $\gamma_0 = 6.2 \times 10^{-4}$ at 15% RH rising to 9.4×10^{-4} at 70% RH for Saharan dust. These values are by nearly 1 order of magnitude higher than those measured in the present study on ATD, $\gamma_0 = 6.9 \times 10^{-5}$ at 15% RH decreasing to 2.7×10^{-5} at 70% RH. This difference can be partly explained by the chemical composition of the dust samples: for instance, Saharan dust contains less of the inactive SiO_2 (47%) and more of the reactive components such as MgO (∼ 5%) and TiO_2 (∼ 5%) compared with Arizona Test Dust with ∼70%, 1−2% and 0.5−1% of SiO_2, MgO and TiO_2, respectively. Another point concerns the surface area of

dx.doi.org/10.1021/jp409946j | J. Phys. Chem. A 2014, 118, 441−448

the solid substrates considered for the calculations of the uptake coefficients in the two studies. In the present study, the BET surface area was used for calculation of H_2O_2 uptake coefficient on ATD leading to the determination of the lower limit of γ_0. In the study of Pradhan et al.,[16] the particle surface area was calculated using the electrical mobility diameters and assuming that the particles have spherical shape. Calculated in this way, surface area represents a lower limit of the reactive surface and, consequently, leads to the determination of the upper limit of the uptake coefficient. It should be noted that, although the above arguments explain to some extent the rather significant difference in uptake of H_2O_2 on ATD from one side and on authentic dust from another, the reason for the observed opposite RH dependences is uncertain. Clearly additional studies are necessary in order to determine whether this contradiction is true and/or to discern its origin.

To the best of our knowledge, the only study reporting data on the steady state uptake of H_2O_2 on minerals is that of Zhao et al,[18] who, using transmission - Fourier Transform Infrared spectroscopy and high-performance liquid chromatography, investigated the heterogeneous interaction of H_2O_2 with SiO_2 and α-Al_2O_3 particles. The steady state uptake coefficient of H_2O_2 on Al_2O_3 surface was found to decrease from 1.2×10^{-7} to 0.8×10^{-7} with increasing RH in the range 2−21%, being almost constant at higher RH (up to 76%). For the SiO_2 surface, nearly 1 order of magnitude lower values were reported. Direct comparison of these data with those obtained in the present study on ATD surface, $\gamma_{SS} \sim 10^{-5}$ for $[H_2O_2]_0 \cong 1.0 \times 10^{12}$ molecules cm^{-3}, is quite difficult regarding the dependence of γ_{SS} on initial concentration of H_2O_2 and its possible dependence on exposure time. It should be noted that typical concentration of H_2O_2 in the study of Zhao et al.[18] was rather high ($\cong 2.4 \times 10^{14}$ molecules cm^{-3}), although no dependence of γ_{SS} on initial concentration of H_2O_2 was observed for $[H_2O_2]_0$ varied in the range $(0.3-3.4) \times 10^{14}$ molecules cm^{-3}. In contrast, in the present study working with much lower concentrations of H_2O_2 ($(0.18 - 5.1) \times 10^{12}$ molecules cm^{-3}), we have observed an inverse dependence of γ_{SS} on concentration of H_2O_2, $\gamma_{ss} \sim [H_2O_2]^{-0.6}$.

The observation of a steady state uptake indicates that uptake of hydrogen peroxide to ATD is a catalytic process and is not limited by site-filling. This observation is in agreement with the conclusions of Wang et al.[17] on a catalytic effect of the mineral oxides on the decomposition of H_2O_2. Catalytic decomposition of H_2O_2 and a small amount of H_2O_2 molecularly adsorbed on the Al_2O_3 particle surface were also reported by Zhao et al.[18] These authors proposed a mechanism for catalytic decomposition of H_2O_2 on Al_2O_3 surface, which includes reactions of gaseous and adsorbed H_2O_2 with surface OH groups, O and Al sites, and involves adsorbed HO_2 radicals as reaction intermediates. The most probable final products of the heterogeneous decomposition of H_2O_2 are O_2 and H_2O. Indeed, Wang et al.[17] reported a release to the gas phase of one O_2 molecule per 2.5 molecules of H_2O_2 consumed on Fe_2O_3 surface. Unfortunately, detection of the potential reaction products in our experimental system was complicated by the presence of relatively high residual concentrations of O_2 and H_2O (from H_2O_2 source) in the reactor.

The atmospheric lifetime, τ_{het}, of H_2O_2 molecules due to the heterogeneous loss onto an aerosol surface can be calculated as

$$\tau_{het} = \frac{1}{k'_{het}} = \frac{4}{\gamma \omega A}$$

where k'_{het} is the first-order rate coefficient of the heterogeneous loss of H_2O_2 (s^{-1}), γ is the uptake coefficient, ω is the mean molecular velocity (cm s^{-1}), and A the aerosol surface area density (cm^2 cm^{-3}). In previous studies,[15,17,19,22] the initial uptake coefficient of H_2O_2 was used for the estimation of τ_{het}. However, the steady state uptake coefficients are more relevant for atmospheric modeling of the reactivity of the aged mineral dust particles. In the present study, RH (2−69%) and temperature (268−320K) independent steady state uptake coefficient, $\gamma_{SS}(dark) = (0.95 \pm 0.30) \times 10^{-5} \times [H_2O_2]^{-0.6}$ (concentration in 10^{12} molecules cm^{-3} units), was measured with H_2O_2 concentration varied in the range $(0.18 - 5.1) \times 10^{12}$ molecules cm^{-3}. For the lowest concentration of H_2O_2 used in the study ($\approx$ 7 ppb at 1 atm), $\gamma_{ss}(dark) \approx 2.7 \times 10^{-5}$. Potentially, at lower tropospheric concentrations of H_2O_2 the value of γ_{SS} can be higher, however, not higher than γ_0, which ranges between 5.8 and 2.7×10^{-5} at RH = 20−70%. Based on this reasoning, a conservative (RH, T, and $[H_2O_2]$ independent) value of $\gamma_{SS} \approx (4.2 \pm 1.5) \times 10^{-5}$ can be recommended from this work for atmospheric implications. Using this value of γ_{SS} and a dust surface loading of $\sim 10^{-6}$ cm^2 cm^{-3}[13,33] the calculated lifetime of H_2O_2 with respect to heterogeneous loss is estimated to be approximately 25 days, i.e., much higher than the photolysis lifetime of H_2O_2 of ∼1 day, which indicates that heterogeneous loss does not represent a significant sink for H_2O_2 compared with its photolysis. However, under specific conditions, for example, of severe dust storm, when aerosol surface loading can be as high as 2×10^{-5} cm^2 cm^{-3}[33] the heterogeneous removal of H_2O_2 (atmospheric lifetime of ≈1.3 day) may be comparable with that due to H_2O_2 photolysis. It has to be emphasized that the lower limit of the uptake coefficient (measured applying BET surface area) was used in the above calculations, i.e., the lifetime of H_2O_2 with respect to its heterogeneous loss may be even shorter. In addition, an appreciable effect of UV irradiation on steady state uptake of H_2O_2 on ATD was observed in the present study: γ_{SS} increased by a factor of 2 under $J_{NO2} = 0.012$ s^{-1}. This means that even higher values of $\gamma_{SS}(UV)$ can be expected on authentic dusts with higher TiO_2 content. In this respect, additional measurements of the steady state uptake coefficient of H_2O_2 on real atmospheric dust samples under UV irradiation are required for more precise assessment of the atmospheric importance of H_2O_2 uptake to mineral aerosol.

AUTHOR INFORMATION

Corresponding Author

*Tel.: +33 238255474; Fax: +33 238696004; e-mail: yuri.bedjanian@cnrs-orleans.fr.

Notes

The authors declare no competing financial interest.

ACKNOWLEDGMENTS

This study was supported by ANR from a Photodust grant. A.E.Z. is very grateful to région Centre for financing his Ph.D. grant.

REFERENCES

(1) Andreae, M. O.; Rosenfeld, D. Aerosol−Cloud−Precipitation Interactions. Part 1. The Nature and Sources of Cloud-Active Aerosols. *Earth-Sci. Rev.* **2008**, *89*, 13−41.

(2) Kanatani, K. T.; Ito, I.; Al-Delaimy, W. K.; Adachi, Y.; Mathews, W. C.; Ramsdell, J. W. Desert Dust Exposure is associated with

Increased Risk of Asthma Hospitalization in Children. *Am. J. Respir. Crit. Care Med.* **2010**, *182*, 1475−1481.
(3) Usher, C. R.; Michel, A. E.; Grassian, V. H. Reactions on Mineral Dust. *Chem. Rev.* **2003**, *103*, 4883−4940.
(4) Dentener, F. J.; Carmichael, G. R.; Zhang, Y.; Lelieveld, J.; Crutzen, P. J. Role of Mineral Aerosol as a Reactive Surface in the Global Troposphere. *J. Geophys. Res.* **1996**, *101*, 22869−22889.
(5) Kolb, C. E.; Cox, R. A.; Abbatt, J. P. D.; Ammann, M.; Davis, E. J.; Donaldson, D. J.; Garrett, B. C.; George, C.; Griffiths, P. T.; Hanson, D. R.; et al. An Overview of Current Issues in the Uptake of Atmospheric Trace Gases by Aerosols and Clouds. *Atmos. Chem. Phys.* **2010**, *10*, 10561−10605.
(6) Lee, M.; Heikes, B. G.; O'Sullivan, D. W. Hydrogen Peroxide and Organic Hydroperoxide in the Troposphere: A Review. *Atmos. Environ.* **2000**, *34*, 3475−3494.
(7) Reeves, C. E.; Penkett, S. A. Measurements of Peroxides and What They Tell Us. *Chem. Rev.* **2003**, *103*, 5199−5218.
(8) Logan, J. A.; Prather, M. J.; Wofsy, S. C.; McElroy, M. B. Tropospheric Chemistry: A Global Perspective. *J. Geophys. Res.* **1981**, *86*, 7210−7254.
(9) Kleinman, L. I. Seasonal Dependence of Boundary Layer Peroxide Concentration: The Low and High NO_x Regimes. *J. Geophys. Res.* **1991**, *96*, 20721−20733.
(10) Jacob, P.; Klockow, D. Hydrogen peroxide measurements in the marine atmosphere. *J. Atmos. Chem.* **1992**, *15*, 353−360.
(11) O'Sullivan, D. W.; Heikes, B. G.; Lee, M.; Chang, W.; Gregory, G. L.; Blake, D. R.; Sachse, G. W. Distribution of Hydrogen Peroxide and Methylhydroperoxide over the Pacific and South Atlantic Oceans. *J. Geophys. Res.* **1999**, *104*, 5635−5646.
(12) Hua, W.; Chen, Z. M.; Jie, C. Y.; Kondo, Y.; Hofzumahaus, A.; Takegawa, N.; Chang, C. C.; Lu, K. D.; Miyazaki, Y.; Kita, K.; et al. Atmospheric Hydrogen Peroxide and Organic Hydroperoxides During Pride-Prd'06, China: Their Concentration, Formation Mechanism and Contribution to Secondary Aerosols. *Atmos. Chem. Phys.* **2008**, *8*, 6755−6773.
(13) De Reus, M.; Fischer, H.; Sander, R.; Gros, V.; Kormann, R.; Salisbury, G.; Van Dingenen, R.; Williams, J.; Zöllner, M.; Lelieveld, J. Observations and Model Calculations of Trace Gas Scavenging in a Dense Saharan Dust Plume during MINATROC. *Atmos. Chem. Phys.* **2005**, *5*, 1787−1803.
(14) Mao, J.; Jacob, D. J.; Evans, M. J.; Olson, J. R.; Ren, X.; Brune, W. H.; Clair, J. M. S.; Crounse, J. D.; Spencer, K. M.; Beaver, M. R.; et al. Chemistry of Hydrogen Oxide Radicals (HO_x) in the Arctic Troposphere in Spring. *Atmos. Chem. Phys.* **2010**, *10*, 5823−5838.
(15) Pradhan, M.; Kalberer, M.; Griffiths, P. T.; Braban, C. F.; Pope, F. D.; Cox, R. A.; Lambert, R. M. Uptake of Gaseous Hydrogen Peroxide by Submicrometer Titanium Dioxide Aerosol as a Function of Relative Humidity. *Environ. Sci. Technol.* **2010**, *44*, 1360−1365.
(16) Pradhan, M.; Kyriakou, G.; Archibald, A. T.; Papageorgiou, A. C.; Kalberer, M.; Lambert, R. M. Heterogeneous Uptake of Gaseous Hydrogen Peroxide by Gobi and Saharan Dust Aerosols: A Potential Missing Sink for H_2O_2 in the Troposphere. *Atmos. Chem. Phys.* **2010**, *10*, 7127−7136.
(17) Wang, W.-g.; Ge, M.-f.; Sun, Q. Heterogeneous Uptake of Hydrogen Peroxide on Mineral Oxides. *Chin. J. Chem. Phys.* **2011**, *24*, 515−520.
(18) Zhao, Y.; Chen, Z.; Shen, X.; Zhang, X. Kinetics and Mechanisms of Heterogeneous Reaction of Gaseous Hydrogen Peroxide on Mineral Oxide Particles. *Environ. Sci. Technol.* **2011**, *45*, 3317−3324.
(19) Zhou, L.; Wang, W.-G.; Ge, M.-F. Temperature Dependence of Heterogeneous Uptake of Hydrogen Peroxide on Silicon Dioxide and Calcium Carbonate. *J. Phys. Chem. A* **2012**, *116*, 7959−7964.
(20) Zhao, Y.; Chen, Z.; Shen, X.; Huang, D. Heterogeneous Reactions of Gaseous Hydrogen Peroxide on Pristine and Acidic Gas-Processed Calcium Carbonate Particles: Effects of Relative Humidity and Surface Coverage of Coating. *Atmos. Environ.* **2013**, *67*, 63−72.
(21) Romanias, M. N.; El Zein, A.; Bedjanian, Y. Heterogeneous Interaction of H_2O_2 with TiO_2 Surface under Dark and UV Light Irradiation Conditions. *J. Phys. Chem. A* **2012**, *116*, 8191−8200.
(22) Romanias, M. N.; El Zein, A.; Bedjanian, Y. Uptake of hydrogen peroxide on the surface of Al_2O_3 and Fe_2O_3. *Atmos. Environ.* **2013**, *77*, 1−8.
(23) Karagulian, F.; Santschi, C.; Rossi, M. J. The Heterogeneous Chemical Kinetics of N_2O_5 on $CaCO_3$ and Other Atmospheric Mineral Dust Surrogates. *Atmos. Chem. Phys.* **2006**, *6*, 1373−1388.
(24) Crowley, J. N.; Ammann, M.; Cox, R. A.; Hynes, R. G.; Jenkin, M. E.; Mellouki, A.; Rossi, M. J.; Troe, J.; Wallington, T. J. Evaluated Kinetic and Photochemical Data for Atmospheric Chemistry: Volume V - heterogeneous reactions on solid substrates. *Atmos. Chem. Phys.* **2010**, *10*, 9059−9223.
(25) Lelièvre, S.; Bedjanian, Y.; Pouvesle, N.; Delfau, J. L.; Vovelle, C.; Le Bras, G. Heterogeneous Reaction of Ozone with Hydrocarbon Flame Soot. *Phys. Chem. Chem. Phys.* **2004**, *6*, 1181−1191.
(26) El Zein, A.; Bedjanian, Y. Interaction of NO_2 with TiO_2 Surface under UV Irradiation: Measurements of the Uptake Coefficient. *Atmos. Chem. Phys.* **2012**, *12*, 1013−1020.
(27) Gershenzon, Y. M.; Grigorieva, V. M.; Ivanov, A. V.; Remorov, R. G. O_3 and OH Sensitivity to Heterogeneous Sinks of HO_x and CH_3O_2 on Aerosol Particles. *Faraday Discuss* **1995**, *100*, 83−100.
(28) Gershenzon, Y. M.; Grigorieva, V. M.; Zasypkin, A. Y.; Remorov, R. G. "Theory of radial diffusion and First Order Wall Reaction in Movable and Immovable Media"; Proceedings of the 13th International Symposium on Gas Kinetics, 1994, Dublin, Ireland.
(29) Underwood, G. M.; Li, P.; Usher, C. R.; Grassian, V. H. Determining Accurate Kinetic Parameters of Potentially Important Heterogeneous Atmospheric Reactions on Solid Particle Surfaces with a Knudsen Cell Reactor. *J. Phys. Chem. A* **2000**, *104*, 819−829.
(30) Goodman, A. L.; Bernard, E. T.; Grassian, V. H. Spectroscopic Study of Nitric Acid and Water Adsorption on Oxide Particles: Enhanced Nitric Acid Uptake Kinetics in the Presence of Adsorbed Water. *J. Phys. Chem. A* **2001**, *105*, 6443−6457.
(31) Ma, Q.; He, H.; Liu, Y. In Situ Drifts Study of Hygroscopic Behavior of Mineral Aerosol. *J. Environ. Sci.* **2010**, *22*, 555−560.
(32) Kraus, A.; Hofzumahaus, A. Field Measurements of Atmospheric Photolysis Frequencies for O_3, NO_2, HCHO, CH_3CHO, H_2O_2, and HONO by UV Spectroradiometry. *J. Atmos. Chem.* **1998**, *31*, 161−180.
(33) Zhang, Y.; Carmichael, G. R. The Role of Mineral Aerosol in Tropospheric Chemistry in East Asia—A Model Study. *J. Appl. Meteorol.* **1999**, *38*, 353−366.